# Technical Communication

## A Preliminary Examination of the Low-Frequency Ambient Noise Field in the South China Sea During the 2001 ASIAEX Experiment

Ruey-Chang Wei, Chi-Fang Chen, Arthur E. Newhall, James F. Lynch, Timothy F. Duda, Chih-Sheng Liu, and Po-Chang Lin

***Abstract*—This correspondence presents a preliminary examination of the low frequency ambient noise field measured in the South China Sea component of the Asian Seas International Acoustics Experiment (ASIAEX), concentrating on the frequencies of 50, 100, 200, 400, 800, and 1200 Hz. A two-week-long time series of the noise at these frequencies is examined for structure in both the time and frequency domains. Three features of particular interest in these series are: 1) the noise due to a typhoon, which passed near the experimental site, 2) the weak tidal frequency variability of the noise field, which is probably due to internal tide induced variability in the propagation conditions, and 3) the vertical angle dependence of the noise, particularly as regards the shallow water "noise notch" phenomenon. The acoustic frequency dependence and the vertical dependence of the noise field are also examined over the course of the time series. A simple look at the noise variability statistics is presented. Finally, directions for further analysis are discussed.**

### I. Introduction

Low-frequency (10–1000 Hz) ambient noise in shallow water has been examined by researchers for over a half a century at this point in time, so its general characteristics are reasonably well understood. We refer the interested reader to the recent text by Katznelson and Petnikov [1] for a brief overview of this topic, along with its substantial list of references.

Due to the occurrence of two very strong atmospheric and oceanic processes at the ASIAEX South China Sea (SCS) site, the ambient noise field measured there has some interesting characteristics, above and beyond the usual ones. Specifically, typhoon Cimaron and the very strong nonlinear internal wave field in the area measurably affected the noise field. It will be the effects of these phenomena on the spatial and temporal characteristics of the noise field that we will concentrate on in this paper.

Our paper is organized as follows. Following this introduction, we will present the experimental background of the ASIAEX SCS experiment, with emphasis on the environmental observations and acoustic noise observations. We will then present the noise time series observations and their associated power spectra. Next, we will examine the vertical distribution of the noise versus time and present a vertical beamforming study. Finally, we will present our results and conclusions.

This work was supported by the U.S. Office of Naval Research under Grants N0001498-1-0413, N00014-00-0931, and N00014-01-0772 and by the NSC of Taiwan under Grant NSC92-2611-E110-004-CCS. This is WHOI contribution number 10996.

R.-C. Wei, C.-S. Liu, and P.-C. Lin are with the National Sun-Yat Sen University, Kaohsiung, Taiwan.

C.-F. Chen is with the National Taiwan University, Taipei, Taiwan.

A. E. Newhall, J. F. Lynch, and T. F. Duda are with the Woods Hole Oceanographic Institution (WHOI), Woods Hole, MA 02543 USA.

Digital Object Identifier 10.1109/JOE.2004.836999

### II. Environmental and Acoustics Measurements—An Overview

As part of the ASIAEX South China Sea experiment, a combined vertical and horizontal acoustic receiving array was deployed in 124 m of water at a site on the Asian continental shelfbreak to the southeast of Hong Kong, at coordinates 21° 52 min N and 117° 11 min E. This array sampled at 3255.208 Hz, allowing it to monitor both experimental signals and noise at half this sampling frequency (the Nyquist criterion). The characteristics of the 32 element horizontal line array (HLA) will not be discussed in this paper—all the measurements we report here will be from the 16 element vertical line array (VLA). (Due to the strong nonlinear internal tides, the horizontal array was dragged across the bottom, which made beamforming with this array more problematical. Moreover, this dragging also created additional, unwanted noise, which has to be filtered from the usual environmental noise found in the ocean waveguide. Thus we have delayed consideration of the data from this array.) The vertical line array had an aperture of 78.75 m occupying the lower 2/3 of the water column at the VLA site. Our original deployment site for the array was in 90 m water depth, which would have let the array fill the water column almost completely, but strong fishing activity at that isobath drove us to deeper water. The 16 vertical hydrophones were not evenly spaced. Rather, the bottom six phones were spaced at 7.5 m intervals and the top ten phones were spaced at 3.75 m intervals.

The array was deployed on May 2, 2001 and recovered on May 18, 2001. Thus, we were able to gather over two weeks (16 days) of acoustic data, which encompassed a full spring-neap tidal cycle (14 days). This was one of the desired objectives of the experiment. In sampling the noise, we had to be careful to record in between the numerous signals that were projected as part of the ASIAEX experiment. A spectrogram of source signals during a rather active period in ASIAEX is shown in Fig. 1, showing some of the signals we needed to avoid when processing the noise. We also have deleted some strong signals due to nearby shipping, "dynamite fishing" and shackle clanging as part of this present analysis. Thus the time series we present will be due to environmental effects and distant shipping.

As a number of papers in this collection have dealt with the strong internal wave field in the ASIAEX SCS area [2], [3], we will not endeavor to repeat their contents—rather we will merely show the temperature field measured at the vertical line array position, displayed in Fig. 2, and discuss its implications for our noise study. Fig. 2 clearly displays the mixed diurnal-semidiurnal tide typical of the site, as well as the rapid temperature excursions of high-frequency nonlinear internal waves. As the wavelength of the internal tide is of the order of thirty kilometers or more, the low frequency (tidal) component of Fig. 2 can be used as a local sound speed field for the immediate region. Modeling by Fredericks *et al.* [4] as well as by Chen and Liu [5] show that, in the absence of finescale oceanography, this internal tide temperature/sound speed signal would lead to very large tidal period fluctuations in the signals and noise. However, in the presence of soliton internal waves, Fredericks *et al.* [4] have shown (using data from the 1996 PRIMER experiment at the New England shelfbreak) that the spectral energy of the acoustic fluctuations is diffused into higher (oceanographic) frequencies, at the expense of the lower (oceanographic) frequency fluctuations. That is just the situation we encounter with our ASIAEX data, and we will discuss this point in more detail later in the paper.

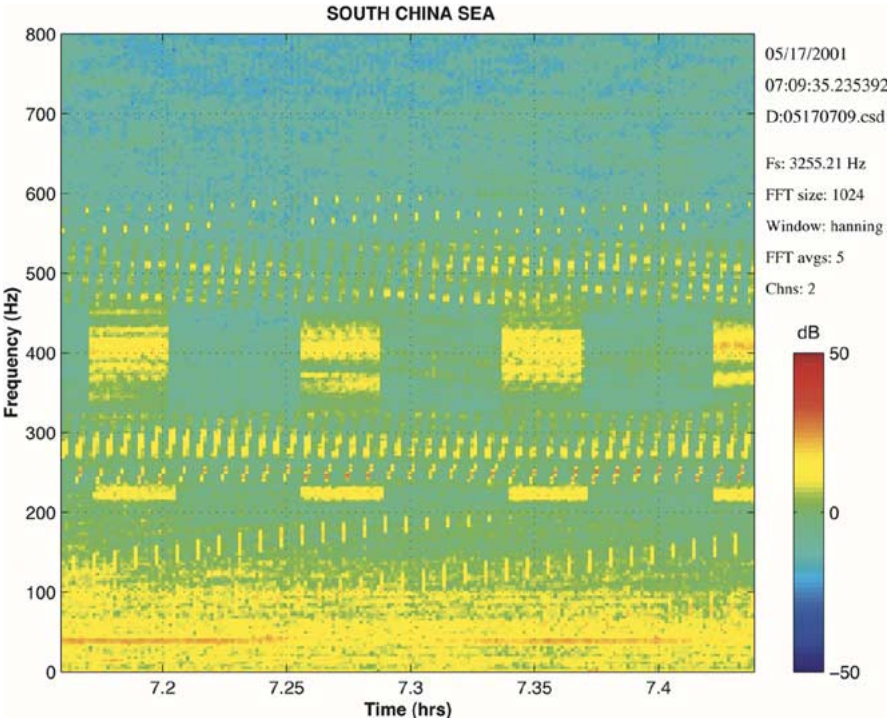


Fig. 1. Spectrogram of transmitted signals during an active period of the ASIAEX South China Sea experimental effort. The noise time series shown in this paper needed to avoid these signals, making processing somewhat time consuming.

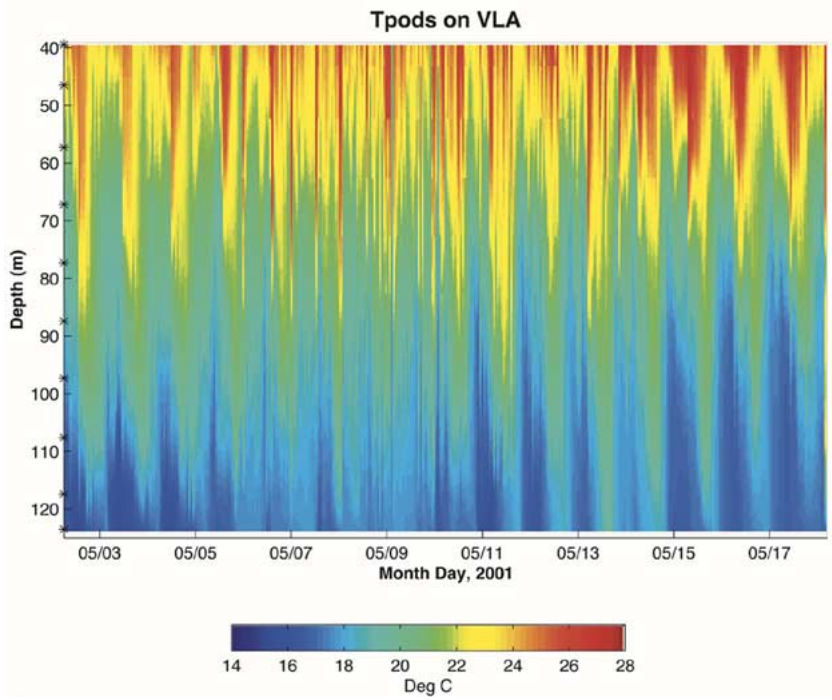


Fig. 2. Temperature records from thermistors attached to the vertical line array acoustic receiver in ASIAEX SCS. Strong diurnal tides, together with some semi-diurnal component, are clearly seen.

A near-seafloor pressure sensor at the 85-m depth site was used to estimate surface gravity wave energy. Bursts of 132 measurements at a sampling rate of 0.5 Hz were recorded every 12 h, providing two wavefield measurements per day. The pressure field for deep-water surface waves (wavelength short compared to water depth) decays as exp(-kz), where $k$ is the wavenumber, so the bottom pressures of the short, high-frequency wind-induced waves are attenuated and not measured. At the depth of our sensor, only waves of period larger than 7 s were measured. Spectral analysis was used to estimate the wave heights in the band spanning periods of 7 to 20 s. Thomson [6] multitaper spec-

tral analysis was performed on each 12-h wave burst and the resulting spectral densities were then corrected for the depth attenuation. After the correction was applied, the rms and/or mean-squared wave heights in the chosen band were computed by integrating the spectrum. The results (Fig. 3) show two time periods with strong waves. Note that there is considerable uncertainty in this computation and the 2.5 m rms may be an overestimate. One strong time period was soon after the deployment, the other was associated with the passage of tropical cyclone Cimaron which is discussed next. The waves in our band were quite small at the other times. It is possible that significant high-frequency waves could have existed at times of weak waves in our measured band. This could occur for a building of local wind with short fetch, with no previously developed longer waves propagating into the measurement site.

The final environmental measurement that we will discuss is that of typhoon Cimaron, which traveled some 430 km to the southeast of our site (at its closest point of approach) during the period 11–14 May, 2001. This track of this modest typhoon is shown in Fig. 4, whereas its winds as measured at Tung-Sha island (just to the east of our site) and at the southern tip of Taiwan are shown in Figs. 5(a) and 5(b). Probably the best approach to recreating the wind-induced surface wave fields is to appeal to large scale numerical meteorological and wave models, inputting the winds measured on land. We have not done this to date, due to the considerable effort involved.

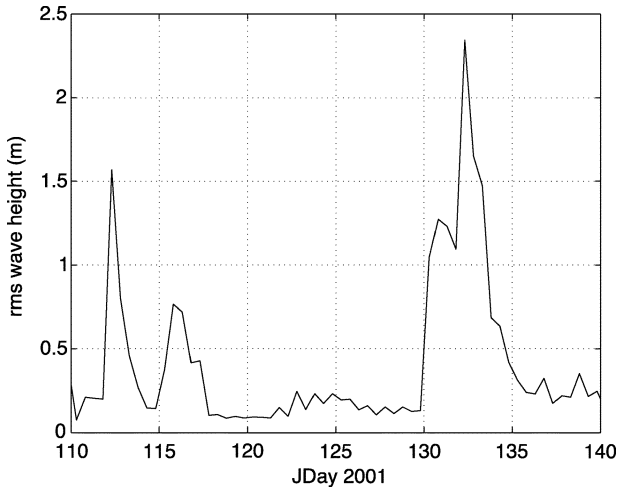


Fig. 3. rms wave height in 7–20 s period band calculated from a pressure sensor at the seafloor at the 85 m site. The time axis is in Julian Day 2001, May 1st, 2001 is JDay 121.

## III. Ambient Noise Time Series and Spectra

Having discussed the background of the noise measurements, we are now ready to examine the noise data themselves. In Fig. 6, we show six panels containing the noise time series at the frequencies of 50, 100, 200, 400, 800, and 1200 Hz. There are two time series shown in each panel. The darker time series is the raw data (actually running averaged over five sampling points to decrease the visual variance of the graph) and the lighter time series is an hourly average of the data, which is useful in examining the effects of tidal and low frequency oceanography on the noise. The levels reported are absolute power spectrum levels in a 1 Hz bandwidth, based on careful calibrations of the receiving hydrophones. The calibration accuracy is estimated to be less than 1 dB in error. The hydrophone used for the Fig. 6 display is hydrophone #1, at water depth 43 m. As we will see, the vertical variability of the noise level is rather small, so that Fig. 6 is a rather representative result.

There are many characteristics of the noise time series in Fig. 6 to consider, some familiar, some novel. The first one, seen by intercomparing the average level of all six panels, is the frequency dependent roll-off of the low frequency noise. This is shown (using daily averages for May 9, 11, and 14 as representative days) in Fig. 7. One sees the familiar decrease of the noise level as frequency increases, reflecting the increasing medium attenuation. This roll-off is found to be independent of the vertical position of the hydrophone, a result that we will state but not explicitly show.

A second interesting feature, perhaps the most prominent one of this data set, is the signature of the typhoon from May 11–14 (or Julian Day 130–133). In all the frequencies in Fig. 6, one sees a slight dip in the noise before day 130, followed by an increase that lasts 2–4 days. These level shifts are rather small (2–3 dB) for the lowest frequencies (50, 100, and 200 Hz), and increase as frequency increases, showing a jump of almost 15 dB at 1200 Hz. Since the typhoon's closest point of approach is over 400 km away from the ASIAEX site, the noise from the core of the typhoon is obviously not heard, no matter how low the frequency. Rather, the wind field (already considerably diminished to a maximum of 7 m/s at Tung-Sha Island) which creates local "wind-seas" and more importantly the distant swell from the storm are responsible for the noise heard. That this noise is generated locally near the receiver is also supported by the greater increase in levels at higher frequencies. Only with a nearby source (order 50 km distance or less) can the highest frequencies be heard.

Another intriguing feature of the typhoon noise signal is the "calm before the storm" that is seen. This effect has the same enhanced sensitivity to higher acoustic frequency as the increase in level after the storm, which suggests that it is related to the same mechanism, which we claim to be local waves. The record of the wind level at Tung-Sha Island shows a lower wind level just before the noise drastically increases, and it also shows that the wind is in the opposite direction to the storm period, which could very easily lay the seas down before the storm. Another possible mechanism for a decrease in noise before the storm is a reduction in fishing boat activity. During Cimaron's passage, the wave level was high enough to discourage small boat activity (such as fishing) at our experimental site, which could also cause a decrease in the noise, particularly at the higher frequencies which are produced by lighter craft. Many craft (including the ASIAEX oceanographic vessels) left the area just before the storm.

A third feature of the time series data, the tidal period variability, is perhaps as subtle to detect as the typhoon event is obvious. Though one can detect an occasional peak in the noise variability with a diurnal or semidiurnal period, the signal is not obvious. Thus we will now turn to the spectral analysis of the time series, which may make such signals clearer. In Fig. 7, we show power spectra of the Fig. 6 time series. Not surprisingly, the spectral peaks at the K1 and M2 tidal frequencies, which are strongly seen in the temperature and pressure field spectra, do not appear strongly above the background except occasionally (see, e.g., the K1 peak at 200 Hz). This result is not unexpected on the basis of past experience. Despite the strong low frequency internal tide signal seen in the thermistor record of Fig. 2 (and thus in the "background" sound speed field), the acoustic scattering by the strong soliton field in the South China Sea "diffuses" the scattering from low oceanographic frequencies into the higher frequencies typical of the soliton field. This is clearly seen both in the time series and their power spectra. This effect has been shown numerically by Fredricks *et al.* [4], who computed propagation fluctuation spectra for an M2 internal tide,

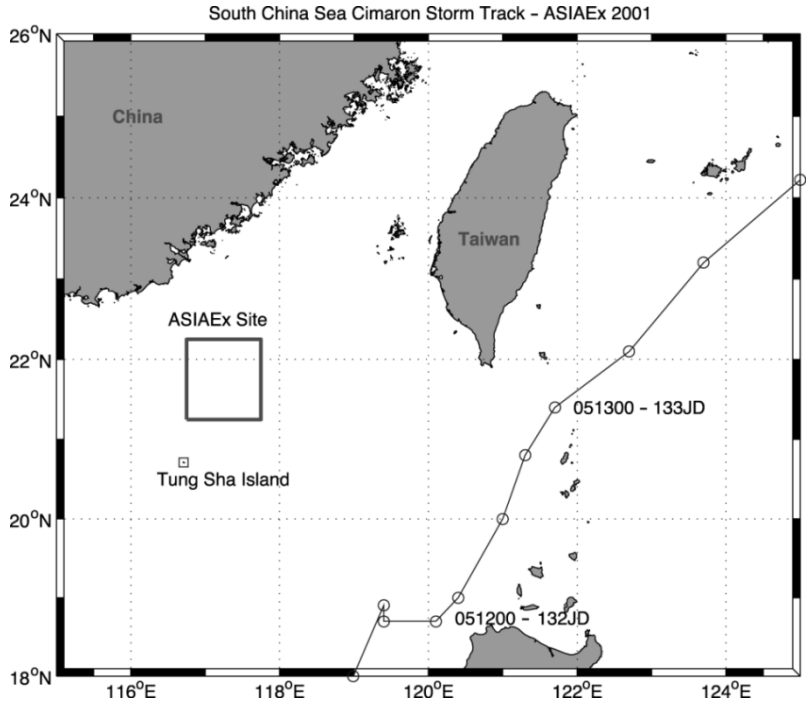


Fig. 4. Storm track of typhoon Cimaron during the 2001 ASIAEX South China Sea experiment. The numbers labeling the two track points are in the order: month, hour, time, and Julian day corresponding to that date/time. The circles in the path denote the typhoon position every six hours.

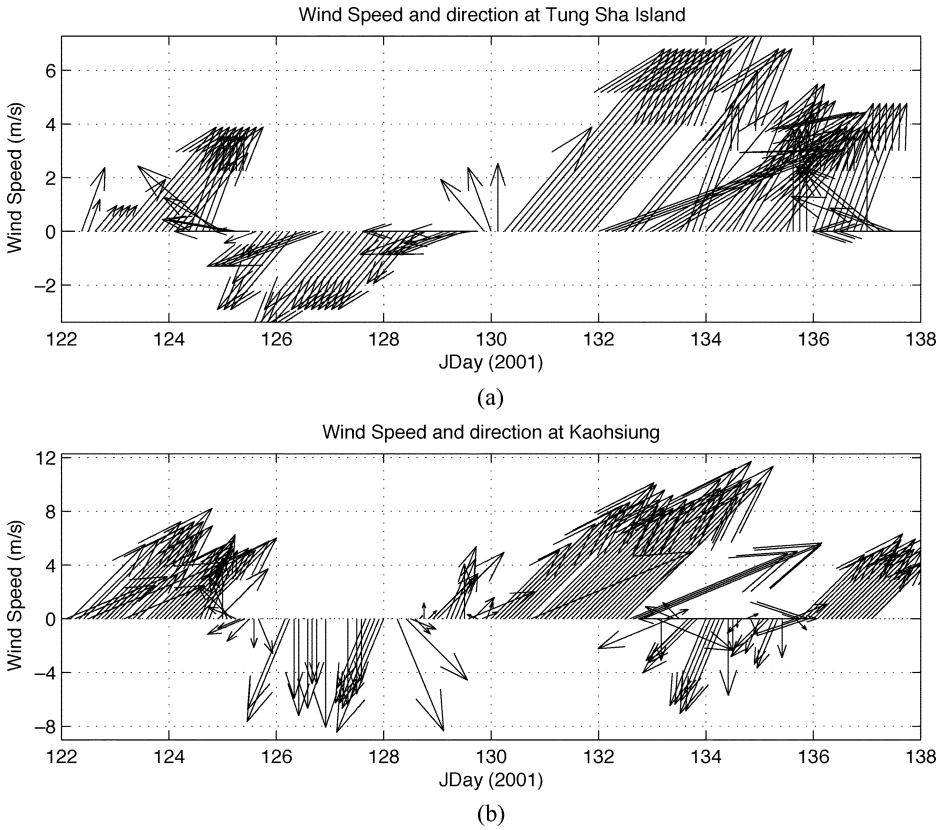


Fig. 5. (a) Wind speed and direction during the ASIAEX SCS experiment as measured a) from Tung-Sha Island (just southwest of the experimental site) and (b) from Kaohsiung (on the southern tip of Taiwan). Both records clearly show the influence of typhoon Cimaron.

with and without solitons present. The fluctuation energy quickly diffused to higher frequencies, and this is probably typical of what one sees in coastal regions with strong soliton fields scattering the acoustic field, such as our ASIAEX site.

## IV. Vertical Dependence of the Noise Field

In Fig. 8(a) and (b), we show the vertical dependence of the noise field at 50 Hz and 1200 Hz, respectively, for five different times on the

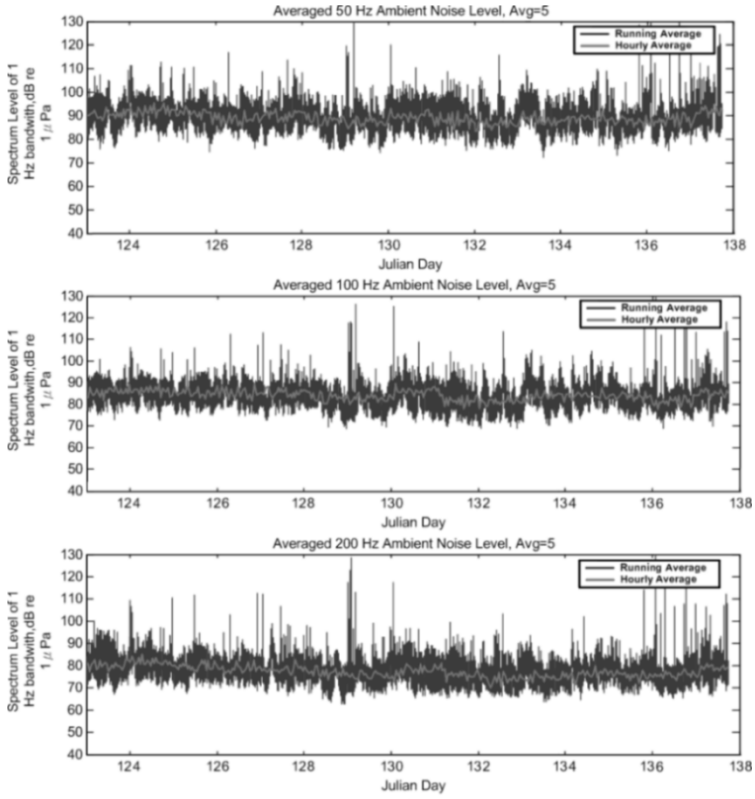


(a)

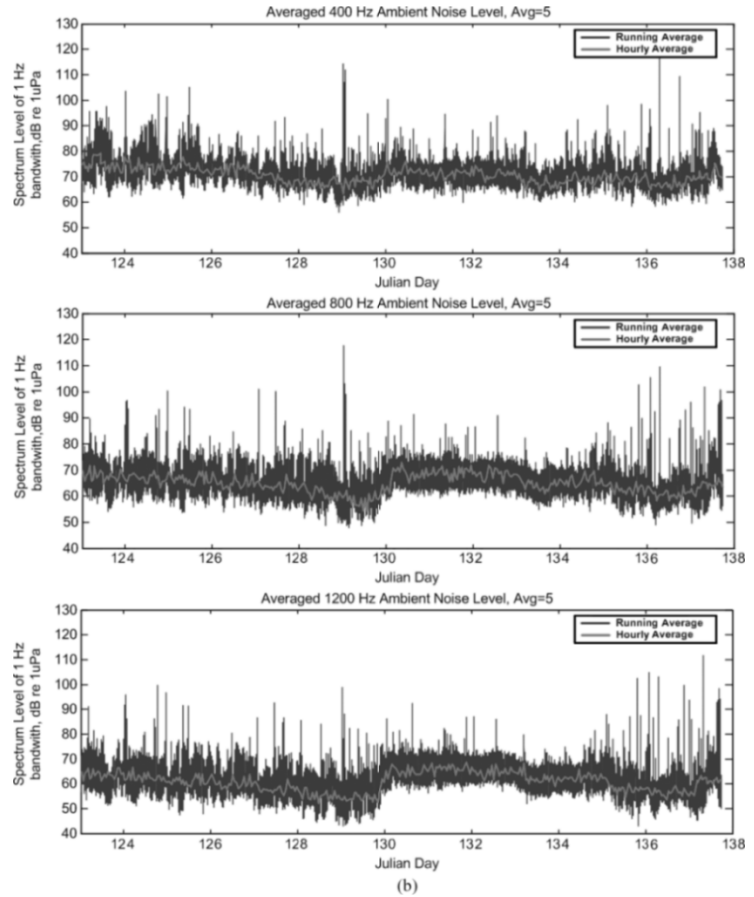


(b)

Fig. 6. (a) Time series of ambient noise at 50, 100, and 200 Hz. (b) Time series of ambient noise at 400, 800, and 1200 Hz. Both five-point averaged and one hour averaged data are shown.

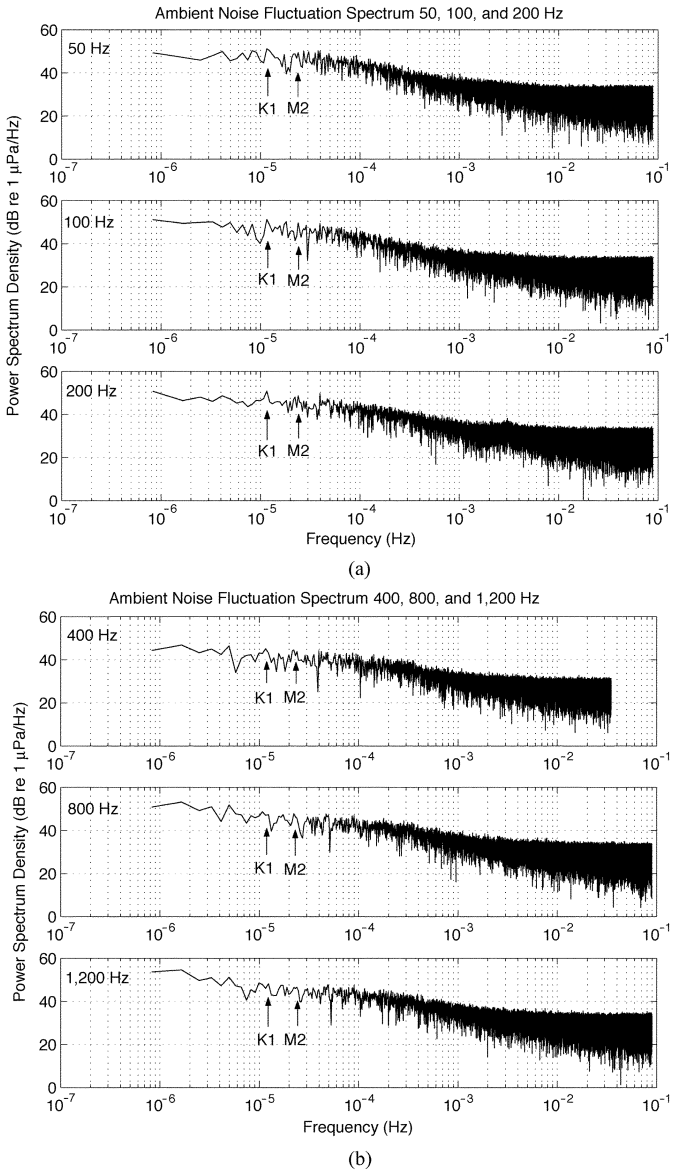


Fig. 7. (a) Spectra of ambient noise at 50, 100, and 200 Hz. (b) Spectra of ambient noise at 400, 800, and 1200 Hz. K1 and M2 tidal frequencies are pointed out in first panel of both (a) and (b).

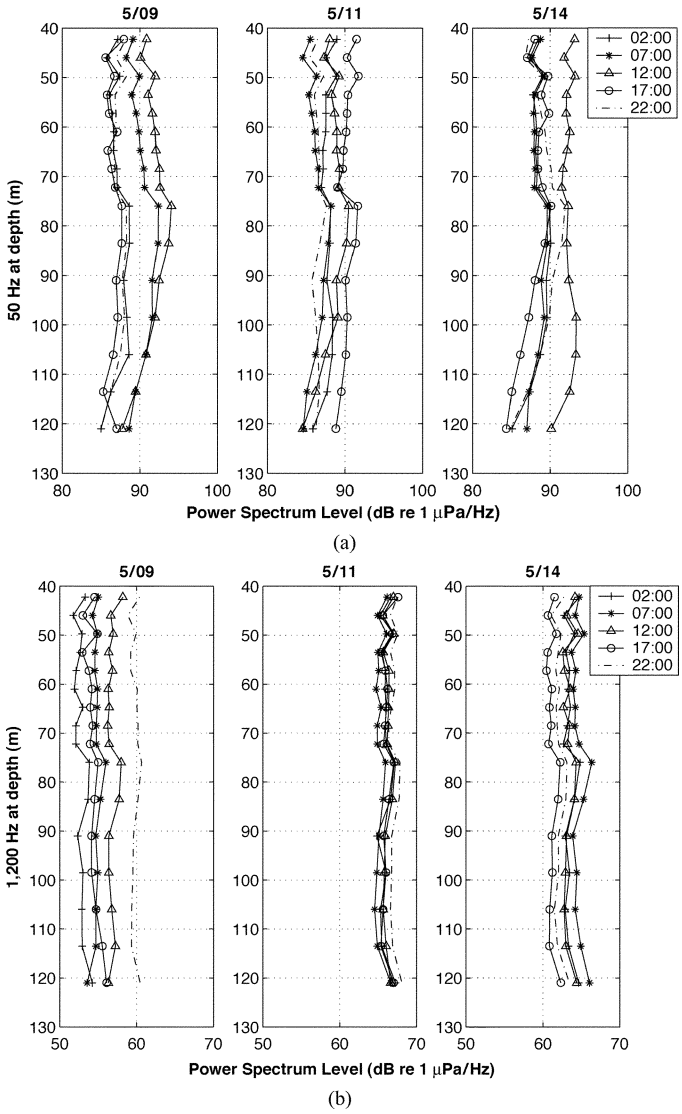


Fig. 8. (a) Vertical dependence of the ambient noise level on three different days and at five different times at 50 Hz. (b) Vertical dependence of the ambient noise level on three different days and at five different times at 1200 Hz.

dates May 9, 11 and 14. It is seen that, while the mean levels change in the vertical, the vertical distribution maintains a fairly constant shape for both the high- and low-frequency noise. Specifically, the low-frequency noise shows a higher level near the sea surface, with a decrease in level toward the bottom. The high-frequency noise shows a much more constant level throughout the water column.

The shape of the low frequency curve is typical of what one expects for surface generated noise in a downward refracting sound speed profile. In that case, the low acoustic normal modes, which ensonify the lower part of the water column, are weakly excited, and so one sees less energy near the bottom. This effect is called the "shallow water noise notch" in the context of sonar systems, and can be examined both in the vertical distribution of the noise (as we do here) and in the angular/modal spectrum of the noise (which is part of our planned beamforming work). We note that this notch occasionally fills in at low frequencies, and can be stronger and weaker. We believe that this is due to solitons scattering energy from the high acoustic modes into the low acoustic modes. We have seen this effect in the New England shelf-break PRIMER experiment [2], and intend to pursue studying it further in the context of the ASIAEX data. Specifically, we will beamform the entire data set so as to examine its modal and angular dependence, and then correlate these against the level of internal wave activity.

The high frequency data should also show a noise notch, but instead show a vertically uniform level, as noted. We hypothesize that this is due to enhanced scattering of the sound by the sound speed perturbation field as frequency increases, which would tend to fill in the noise notch more effectively than at low frequencies. Again, we need to look at the angular and modal distribution of energy after beamforming, and correlate it against internal wave activity, this time with the addition of acoustic frequency as a parameter of interest.

## V. Simple Statistics of the Noise Field

In Fig. 9(a) and (b), we show the mean levels and standard deviations of the noise on three different days versus frequency. The mean level variability of the noise versus frequency has been discussed before, and

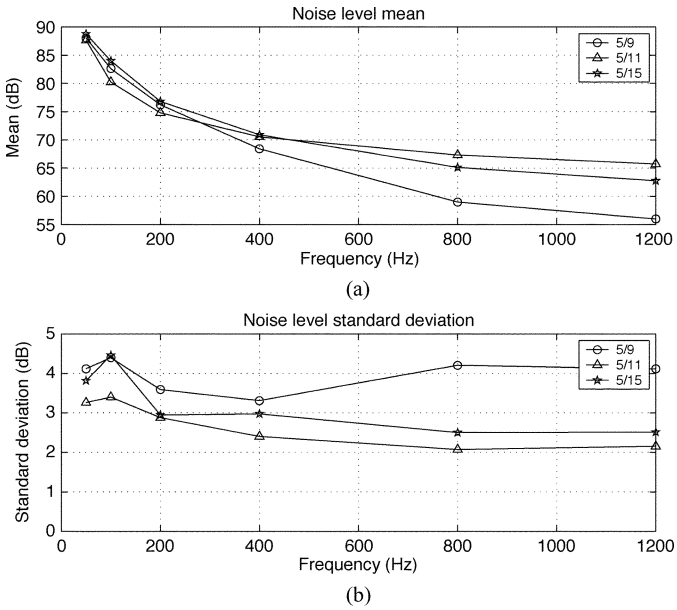


Fig. 9. (a) Mean ambient noise level for three days at 50, 100, 200, 400, 800, and 1200 Hz. (b) Standard deviation of the ambient noise level for three days at 50, 100, 200, 400, 800, and 1200 Hz.

is not surprising. The standard deviation of the noise is also rather constant at 3–4 dB, so that the statistics seem to be rather uninteresting. However, there is one study we are planning that may hold somewhat more interest, which is to look at the variability in the noise versus the oceanographic frequency (i.e. in the subtidal, tidal, and high frequency bands), with a particular emphasis on periods of high and low internal wave activity. This would parallel recent studies by Fredricks *et al.* [4] and Chiu *et al.* (private communication), who examined the fluctuations of both signals and noise as a function of oceanography in the shelfbreak PRIMER experiment, as well as the work by Duda *et al.* [7] and Chiu *et al.* [8], who studied signal fluctuations in the ASIAEX SCS data.

## VI. Vertical Beamforming Studies

Another useful way to examine our noise data is to look at the vertical angular distribution of the data, i.e. "steer" the vertical array to different vertical grazing angles and look at the noise power output. We could alternately "modeform" the data, i.e. look at a matched filter output for the power in the individual normal modes, but have chosen the simpler and more easily interpreted angular beamforming method to examine the vertical angle dependence of the noise. We will make the assumptions that the vertical array is not significantly tilted and that the arrivals are plane waves. Both of these assumptions have some error in them, but we regard the amount of error as tolerable for the current analysis. We have examined the 100 and 200 Hz data using the entire 16 element hydrophone array, but are only using the top ten hydrophones for the 400 and 800 Hz data, since the top ten array elements have different spacing than the elements in the lower portion. We note that due to grating lobes, there is a $\pm 20^\circ$ sector usable at 800 Hz, about $\pm 30^\circ$ sector usable at 200 and 400 Hz, and about a $\pm 40^\circ$ sector usable at 100 Hz. Since power increases outside the those sectors due to sidelobe effects, we will focus all our analyzes within those sectors.

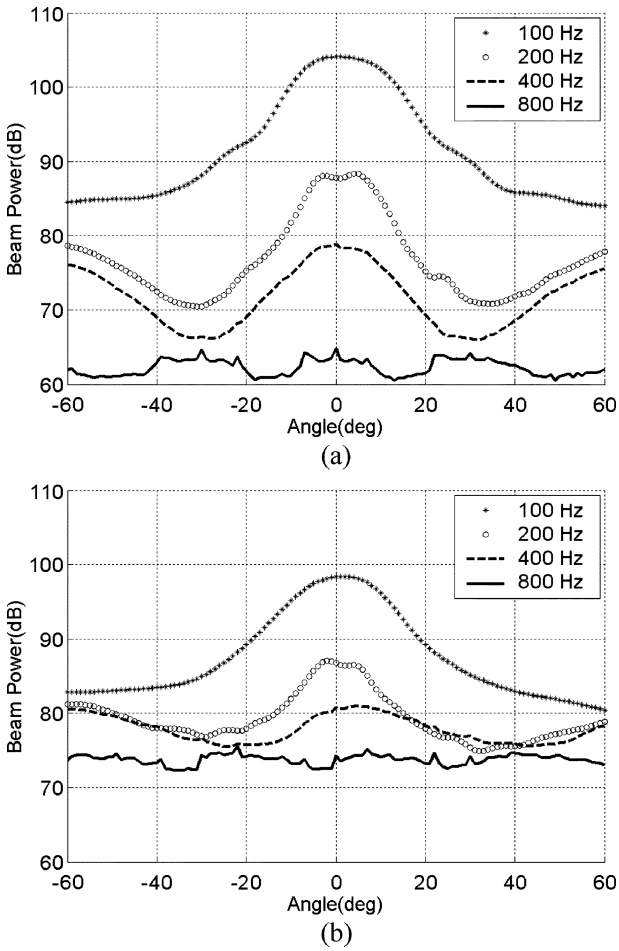


Fig. 10. Vertical distribution of noise after beamforming over angles $\pm 60^\circ$ for four frequencies for a low wind speed case (a) taken on May 11th (JDay 131) at 11:06 (GMT) and a high-wind speed case (b) taken on May 9th (JDay 129) at 11:02 (GMT).

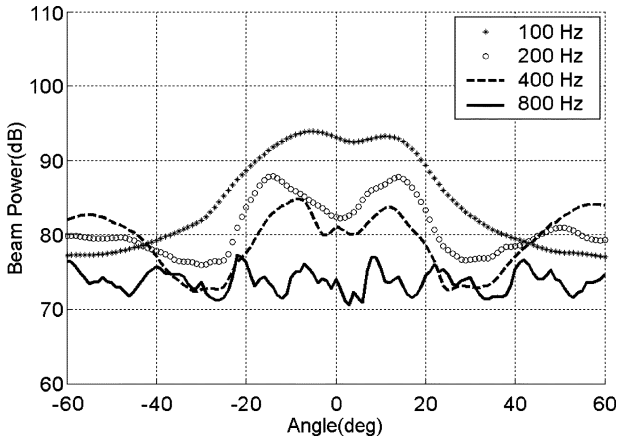


Fig. 11. Vertical distribution of noise after beamforming over angles $\pm 60^\circ$ for four frequencies taken on May 9th (JDay 129) at 22:15 (GMT), for a case when the noise notch effect is apparent.

Using coherent beamforming and averaging the results over two minutes, we show the vertical distribution of noise for the four frequencies we consider for both a low wind speed case [see Fig. 10(a)] and a high-wind speed case [see Fig. 10(b)]. The noise in both cases is concentrated at the low angles, indicating that the low angle "noise notch," caused by the dominance of high angle surface noise, has been

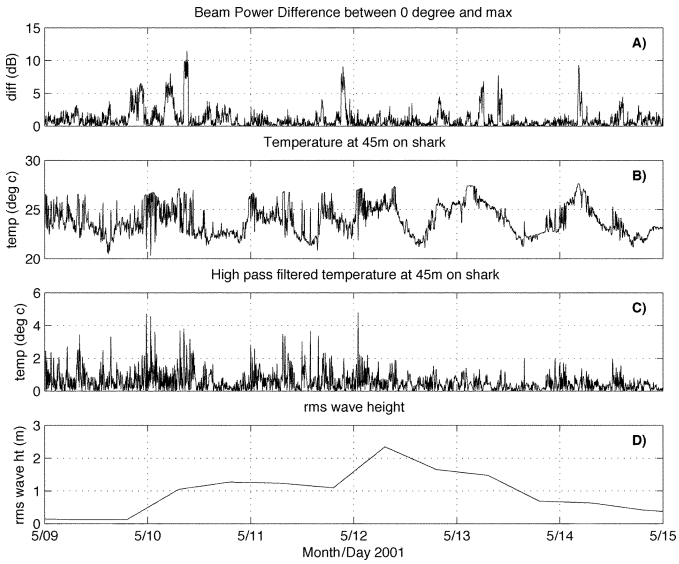


Fig. 12. Time series from 5/09–5/15, 2001 of (a) dB difference between the maximum beam output and the beam output at 0° for 200 Hz noise, i.e., the 200 Hz "noise notch" magnitude, (b) the temperature time series at 45 m on the vertical array acoustic receiver (a measure of the internal wave activity and other oceanography), (c) the high-pass filtered version of the time series in (b), which emphasizes the soliton internal waves, and (d) the rms surface wave height, emphasizing the typhoon period.

countered by scattering of sound into the low angle modes that propagate with less attenuation. This is seen in both the low and high wind speed cases. This is not surprising in the South China Sea, where the intense soliton field creates a strong acoustic mode coupling/scattering mechanism much of the time.

For a large fraction of the time, the noise notch does not appear; however, we also show a case where the noise notch effect does appear. In Fig. 11, we see that the noise notch effect is strong at 200 and 400 Hz, but does not appear to be strong at 100 or 800 Hz. We ascribe this to the frequency dependence of the scattering by the internal waves, but admit that this is only a working hypothesis, and needs further study. Using the empirical observation that the noise notch effect appears to be strongest at 200 Hz, we can consider the power difference between the maximum beam output and the beam output at 0° at 200 Hz to examine the time history of the noise notch at the ASIAEX site over six days [see Fig. 12(a)]. We see that the noise notch has an "intermittent burst" nature, being strong (∼5–10 dB) for a few hours, and then relaxing to small (∼1–2 dB) values the rest of the time, the low values probably being the "noise floor" for our description of the notch.

In that the low-frequency noise is very probably created mostly at the surface by waves during the typhoon swell period (which creates high angle noise for the noise notch effect), and since it is scattered strongly by internal waves (which would fill in the noise notch), it is reasonable to examine whether there is any correlation between the surface waves, the internal waves, and the noise notch. This is done in Fig. 12(a)–(d), which shows: a) the noise notch time series at 200 Hz over the period from 5/09–5/15, 2001, b) the temperature time series at 45 m on the vertical array acoustic receiver (a measure of the internal wave activity and other oceanography), c) the high-pass filtered version of the time series in (b), which emphasizes the soliton internal waves, and d) the rms surface wave height, emphasizing the typhoon period. Though visual inspection gives only a crude measure of cross-correlations between variables, it is rather obvious from Fig. 12 that there are no readily apparent correlations between these simple oceanographic variables and the acoustic noise notch. Our appraisal of this result is that we are probably looking at too simple a set of environmental variables to explain the noise notch formation and dissipation, and that a more complicated factor, incorporating the joint influence of oceanographic and bottom environmental variables, might correlate better to the noise notch. It is in this direction that we intend to look in future work.

## VII. Conclusions and Future Directions

In this paper, we have given the reader a brief look at the ambient noise data from the 2001 ASIAEX SCS experiment. We have seen a number of interesting features in the data, including the signatures of a typhoon and the internal tides. However, our explanations of what causes the features seen in the data are admittedly unproven, and at this point in time, we have only presented what we think are reasonable hypotheses. In order to prove or disprove these hypotheses, much work needs to be done, especially as regards the horizontal beamforming of the data. By beamforming these data, we can eventually find out whether our "local noise generation" and "internal tide scattering" hypotheses are true, and thus understand both the acoustic features presented here, as well as how they correlate to the environmental forcing.

## Acknowledgment

The list of acknowledgment for an experiment such as ASIAEX is necessarily a long one, so just to be safe, we will thank *all* of our sponsors, colleagues, and students for their support, collaboration, hard work, and sense of humor, without which ASIAEX would not have succeeded. In particular, we will single out the ASIAEX coordinators, whose "behind the scenes" efforts cleared the path for the experiment, the captain and crew of the Fisheries Researcher I, which deployed and recovered our acoustic array, our super engineering and buoy deployment teams, which got us the data, and the Grand Jai-Lai Hotel, which made Kaohsiung a "bit-of-heaven" for the foreign visitors.

## References

[1] B. G. Katsnelson and V. G. Petnikov, *Shallow Water Acoustics*: Springer-Verlag, 2002, ch. 7, pp. 189–220.

[2] T. F. Duda, J. F. Lynch, J. D. Irish, R. C. Beardsley, S. Ramp, C. S. Chiu, T. Y. Tang, and Y. J. Yang, "Internal tide and nonlinear internal wave behavior at the continental slope in the northern South China Sea," *IEEE J. Oceanic Eng.*, vol. 29, pp. 1105–1130, Oct. 2004.

[3] S. Ramp, D. Tang, T. F. Duda, J. F. Lynch, A. Liu, C. S. Chiu, F. Bahr, H. R. Kim, and Y. J. Yang, "Internal solitons in the northeastern South China Sea part I: sources and deep water propagation," *IEEE J. Oceanic Eng.*, vol. 29, pp. 1157–1181, Oct. 2004.

[4] A. Fredricks, J. A. Colosi, J. F. Lynch, G. G. Gawarkiewicz, C. S. Chiu, and P. Abbot, "Analysis of multipath scintillations observed during the summer 1996 New England shelfbreak PRIMER study," J. Acoust. Soc. Amer., 2003, submitted for publication.

[5] C. S. Liu, "ASIAEX: A Study of the Background Noise in the South China Sea," Masters Thesis, National Sun-Yat Sen University, Taiwan, Aug. 2003.

[6] D. J. Thomson, "Spectral estimation and harmonic analysis," *Proc. IEEE*, vol. 10, pp. 1055–1096, 1982.

[7] T. F. Duda, J. F. Lynch, A. E. Newhall, L. Wu, and C. S. Chiu, "Fluctuations of 400 Hz sound intensity in the 2001 ASIAEX South China Sea experiment," *IEEE J. Oceanic Eng.*, vol. 29, pp. 1264–1279, Oct. 2004.

[8] C. S. Chiu, S. Ramp, C. W. Miller, J. F. Lynch, T. F. Duda, and T. Y. Tang, "Acoustic intensity fluctuations induced by South China Sea internal tides and solitons," *IEEE J. Oceanic Eng.*, vol. 29, pp. 1249–1263, Oct. 2004.